Deep-Sea Research I 79 (2013) 141–155

Contents lists available at SciVerse ScienceDirect

Deep-Sea Research I

journal homepage: www.elsevier.com/locate/dsri

Spatial and temporal variations in variable fluoresence in the Ross Sea (Antarctica): Oceanographic correlates and bloom dynamics

Walker O. Smith Jr.[a,*], Sasha Tozzi[a,1], Matthew C. Long[b,2], Peter N. Sedwick[c], Jill A. Peloquin[a,3], Robert B. Dunbar[b], David A. Hutchins[d], Zbigniew Kolber[e,1], Giacomo R. DiTullio[f]

[a] Virginia Institute of Marine Science, College of William and Mary, Gloucester Pt., VA 23062, USA
[b] Environmental Earth System Science, Stanford University, Palo Alto, CA 94305, USA
[c] Ocean, Earth & Atmospheric Sciences, Old Dominion University, Norfolk, VA 23529, USA
[d] Department of Biological Sciences, University of Southern California, Los Angeles, CA 90089, USA
[e] Monterey Bay Aquarium Research Institute, Moss Landing, CA 95039, USA
[f] Hollings Marine Laboratory, College of Charleston, Charleston, SC 29412, USA

ARTICLE INFO

Article history:
Received 23 October 2012
Received in revised form
29 April 2013
Accepted 8 May 2013
Available online 30 May 2013

Keywords:
Quantum yield
Photosynthesis
Pigments
Ross Sea
Diatoms
Phaeocystis

ABSTRACT

During two cruises to the Ross Sea, Antarctica in austral spring and summer, fast repetition rate fluorometry was used to investigate the relationship between phytoplankton photophysiology and water mass characteristics, micronutrient availability, and composition. Particulate organic matter proxies for phytoplankton biomass (chlorophyll *a*, particulate organic carbon and nitrogen, and biogenic silica) were all elevated in the photic zone during spring and summer. Biogenic silica concentrations were an order of magnitude higher in summer relative to spring, reflecting a shift in composition from *Phaeocystis antarctica* to diatoms. Quantum yields of PS II (F_v/F_m) were generally higher in spring relative to summer, coincident with weaker vertical and horizontal gradients in hydrographic properties. Reduced F_v/F_m values (<0.4) were observed in the upper 30 m in both seasons, with maximum values (ca. 0.55) observed near base and below the euphotic zone. No significant relationship between F_v/F_m values and dissolved Fe could be identified in the merged spring/summer data set. Functional absorption cross sections were significantly higher in spring than summer, presumably reflecting adaptations to lower irradiance in spring; little variation with depth was observed. Phytoplankton composition did not appear to be a major determinant of bulk quantum yield, although diatom-dominated waters exhibited significantly higher functional absorption cross sections when compared to waters dominated by *P. antarctica*. Dominance of *P. antarctica* appears to be related to greater photophysiological resilience and faster photoacclimation to changing light conditions, whereas diatoms were prevalent in shallow summer mixed layers, which likely reflects their enhanced photosynthetic capacity at high irradiance levels.

1. Introduction

Continental shelves around Antarctica have been recognized as critical sinks for atmospheric carbon dioxide. Indeed, it has been estimated that the Ross Sea continental shelf is responsible for more than 25% of the known Southern Ocean sink for anthropogenic CO_2 (Arrigo et al., 2008). Atmosphere to ocean carbon flux on continental shelves is driven by the incorporation of CO_2 by phytoplankton during the growing season and subsequent vertical export of organic matter to depth. Phytoplankton assemblages in the highly productive continental shelf area of the Ross Sea are dominated by two functional groups: haptophytes and diatoms (Tremblay and Smith, 2007). The haptophytes are overwhelmingly dominated by *Phaeocystis antarctica* (DiTullio et al., 2003), with chlorophyll *a* concentrations of ca. 15 μg L^{-1} being observed in spring, declining to low concentrations by mid-January (Smith et al., 2006, 2011a). *P. antarctica* dominates in relatively deep mixed layers, maintaining high photosynthetic and growth rates despite the reduced irradiance levels characteristic of

* Corresponding author.
E-mail addresses: wos@vims.edu (W.O. Smith Jr.), stozzi@ucsc.edu (S. Tozzi), mclong@ucar.edu (M.C. Long), psedwick@odu.edu (P.N. Sedwick), Jill.peloquin@gmail.com (J.A. Peloquin), dunbar@stanford.edu (R.B. Dunbar), dahutch@usc.edu (D.A. Hutchins), zkolber@ucsc.edu (Z. Kolber), ditullioj@cofc.edu (G.R. DiTullio).
[1] Present address: Institute of Marine Sciences, University of California, Santa Cruz, Santa Cruz, CA 95064, USA.
[2] Present address: National Center for Atmospheric Research, Boulder, CO 80305, USA.
[3] Present address: Institute for Biogeochemistry and Pollutant Dynamics Federal Institute of Technology, Zürich.

0967-0637/$ - see front matter © 2013 Elsevier Ltd. All rights reserved.
http://dx.doi.org/10.1016/j.dsr.2013.05.002

austral spring (Arrigo et al., 1999; Smith et al., 2000). In contrast, diatoms typically flourish during summer, and dominate regions within shallow mixed layers (such as those near ice edges), efficiently harnessing the elevated photon fluxes for photosynthesis (Leventer and Dunbar, 1996; Kropuenske et al., 2009). In addition to blooming in different oceanographic conditions, *P. antarctica* and diatom populations have substantially different elemental stoichiometry, which in turn impacts the magnitude and elemental compositon of the vertical export flux on the continental shelf (Dunbar et al., 2003). It remains unclear whether the specific physiological characteristics of the two functional groups result in dominance at any particular point in time, or the relative importance of micronutrients and irradiance in controlling phyiological characteristics of the algae.

Low iron concentrations have been shown to limit phytoplankton growth in much of the Southern Ocean (Martin et al., 1990a; de Baar et al., 1999; Boyd et al., 2000; Alderkamp et al., 2012b), including the Ross Sea (Martin et al., 1990b; Sedwick and DiTullio, 1997; Sedwick et al., 2000; Olson et al., 2000). Convective overturn during the fall and winter replenishes Fe in surface waters and leaves the early spring water column weakly stratified; thus, irradiance is thought to limit phytoplankton growth and productivity during this season (Smith et al., 2000). However, recent work indicates that dissolved iron concentrations can also be low in the Ross Sea polynya during spring (Sedwick et al., 2011), suggesting that biological iron drawdown early in the season can create iron-limited conditions earlier than had been previously thought. Iron, an essential component of phytoplankton photosynthetic machinery and of other enzymes, such as nitrate reductase, is supplied to the euphotic zone by upwelling of subsurface, relatively iron-rich deep waters, winter convective mixing, melting of sea ice and atmospheric deposition (Sedwick et al., 2000, 2011; Measures and Vink, 2001; Dinniman et al., 2003, 2011).

P. antarctica populations dominate in more deeply mixed water columns, whereas diatoms tend to dominate in more highly stratified waters (Arrigo et al., 1999, 2003; Smith and Asper, 2001). However, the habitats of these two groups overlap, and no statistically significant difference has been demonstrated between mixed layer depths or photosynthetic parameters in waters dominated by either haptophytes or diatoms (van Hilst and Smith, 2002). Furthermore, the limited dissolved iron distribution and cycling data for the Ross Sea do not allow generalizations with regard to the concentrations of dissolved iron in deeply mixed versus stratified waters, given that both vertical mixing and sea-ice melting are thought to supply iron to surface waters in this region (Sedwick et al., 2000, 2011; Coale et al., 2005). In this context, direct observations of the photophysiological status of phytoplankton should provide information on the apparent habitat differentiation between *P. antarctica* and diatoms in the Ross Sea.

Variable fluorescence has been widely used as a method for assessing the photochemical status and response of phytoplankton to a variety of factors, including deficiencies in macro- and micronutrients (Kolber et al., 1994; Behrenfeld and Kolber, 1999; Olson et al., 2000; Parkhill et al., 2001). Hiscock et al. (2007) showed that quantum yields of phytoplankton in the Southern Ocean are responsive to iron availability and suggested that a low quantum yield is indicative of iron stress. One method for measuring variable fluorescence is fast repetition rate fluorometry (FRRF; Kolber et al., 1998). This procedure manipulates the photosystem II (PS II) redox state by reducing the primary electron acceptor with short ($\sim$100 μs) sequences of flashes within a single turnover of the PSII reaction center, allowing assessment of the photosynthetic quantum yield of PSII (F_v/F_m) and the functional absorption cross section of PSII (σ_{PSII}). We conducted an investigation into the controls on phytoplankton photosynthesis, growth and composition during two seasons: early austral summer (December, 2005–January, 2006) and the following spring (November–December, 2006). As part of these cruises, we assessed variable fluorescence distributions within the southern Ross Sea, as well as the relationship among variable fluorescence, phytoplankton assemblage composition, and hydrographic variables. We hypothesized that variations in active fluorescence characteristics would reflect changes in phytoplankton photophysiology and composition, and highlight iron availability as one of the primary factors controlling photosynthetic capacity, which in turn would have a significant impact on phytoplankton quantum yields in the Ross Sea.

2. Materials and methods

All sampling was conducted in the Ross Sea polynya as part of the "Controls on Ross Sea Algal Community Structure (CORSACS)" project during two cruises on the *RVIB Nathaniel B. Palmer* (Cruises NBP06-01, December 2005–January 2006, and NBP06-08, November–December 2006). Results are merged to reflect a seasonal progression due to the changes in ice, the dominant environmental variable, rather than absolute time, as seasonal changes are far

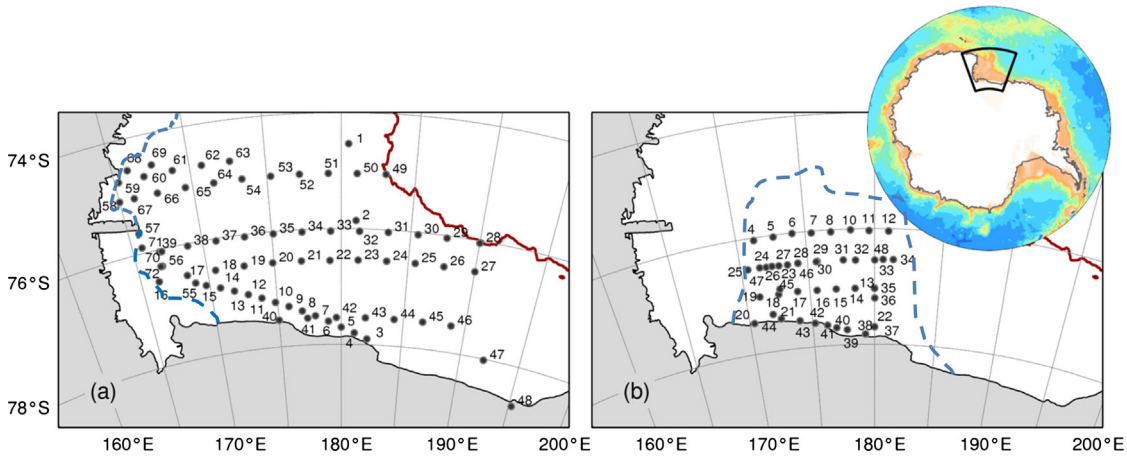

Fig. 1. Map showing the bathymetry of the study area and station locations of *R.V.I.B. N.B. Palmer* cruises (a) NBP06-01 (sampled from December 27, 2005 to January 23, 2006) and (b) NBP06-08 (sampled from November 6 to December 6, 2006). The dashed line on both is the ice distribution at the mid-point of each cruise, and the solid red line is the location of the continental shelf break.

greater than those observed interannually (Smith et al., 2000). Hydrographic properties of the Ross Sea continental shelf were assessed with 102 CTD casts at 74 stations during the summer cruise NBP06-01 and 72 CTD casts at 43 stations during the spring cruise on NBP06-08 (Fig. 1). Five zonal transects (along 74.5°S, 75.0°S, 76.0°S, 76.5°S, and 77.5°S) and a sixth transect parallel to the Ross ice shelf between 168.5°E and 177.8°W were completed during the summer cruise, and four transects (along 76.0°S, 76.5°S, and 77.5°S, as well as one parallel to the ice shelf) were completed during the spring cruise. Conductivity, temperature, and depth were measured using a SeaBird 911+ CTD mounted on an epoxy-coated rosette sampler fitted with 24 10-L Bullister bottles. Mixed layer depths (z_{mix}) were defined as the depth at which σ_t values increased by 0.05 kg m^{-3} from a stable surface value in summer, and by 0.02 kg m^{-3} in spring, when density differences were less pronounced. Surface irradiance was recorded with a Biospherical QSR-240 quantum sensor mounted on the mast above the ship's bridge, and irradiance profiles were measured with a Biospherical QSP 2300 quantum sensor attached above the rosette. Dissolved inorganic nutrients (nitrate, nitrite, phosphate, ammonium and silicic acid) were measured in samples from all depths. Samples for nutrients (60 mL) were collected with an acid-washed syringe and filtered through a 0.2 μm Gelman Acrodisk into 125 mL acid-washed polypropylene bottles. Nutrient analyses were performed at sea on a Lachat QuickChem Autanalyzer using standard automated techniques. Precision on nitrate, nitrite, phosphate, and silicic acid was 5%, and lower limits of detection were 0.05 μM.

Seawater samples for dissolved iron analysis were collected in custom-modified 5-L Teflon-lined, external-closure Niskin-X samplers (General Oceanics Inc.) or 10-L teflon-lined GO-FLO samplers (General Oceanics Inc., for >300 m depth samples only), all of which were deployed on a non-metal line (Sedwick et al., 2011). All samples were filtered within 4 h of collection using pre-rinsed 0.2 μm pore Supor Acropak filter cartridges (Pall Corp.), except for the GO-FLO samples, which were filtered through 0.4 μm pore, 144 mm diameter polycarbonate membranes (GE Osmonics). Filtered samples were acidified to pH 1.7 with ultrapure hydrochloric acid and stored for at least 24 h prior to the analysis of dissolved iron. Dissolved iron was determined by flow injection analysis with colorimetric detection after in-line pre-concentration on resin-immobilized 8-hydroxyquinoline (Sedwick et al., 2008) using a method modified from Measures et al. (1995). The efficacy of these sampling and analytical methods has been verified through participation in the *SAFe* intercomparison exercise for the sampling and analysis of iron in seawater (Johnson et al., 2007). The level of detection for dissolved iron is 0.04 nM and the precision of samples near 0.1 nM is 0.01 nM (Sedwick et al., 2008, 2011).

Samples for chlorophyll *a* (Chl *a*) were collected from the 10-L Niskin bottles into clean, dark polyethylene bottles and immediately filtered through 25 mm GF/F Whatman glass fiber filters (nominal pore size 0.7 μm) using a vacuum <5 psi. Filters were placed in borosilicate tubes with 90% acetone, capped, and extracted in the dark for 24 h at −20 °C (JGOFS,1996). Following extraction, the filters were removed and the chlorophyll *a* quantified by a non-acidification method (Welschmeyer, 1994) using a Turner Designs TD700 fluorometer calibrated at the beginning and end of each cruise using commercially purified chlorophyll *a* (Sigma); 90% acetone served as a fluorometer blank (precision 10%; lowever limit of detection 0.01 μg L^{-1}). Particulate organic carbon (POC) and nitrogen (PON) concentrations were determined for known volumes of water filtered through precombusted (450 °C for 2 h) GFF filters that were rinsed with 5 mL 0.01 N HCl in filtered seawater, placed in combusted glass vials, dried at 60 °C, and analyzed on a Carlo-Erba 1108 elemental analyzer using acetanilide as a standard (Asper and Smith, 1999). Blanks were filters that had ca. 5 mL filtered seawater passed through them and treated as above (precision 10%). Biogenic silica (BSi) samples were filtered onto 0.6 μM polycarbonate filters, dried at 60 °C, and stored at ambient temperature until analysis in the laboratory where BSi was concentrations were determined spectrophotometrically according to Brzezinski and Nelson (1995). Precision for BSi measurements is ca. 5% and the lower limit of detection ca. 0.02 μM.

Pigments were quantified with high performance liquid chromatography according to DiTullio and Geesey (2002). The major pigments measured were chlorophyll *a* (Chl *a*), fucoxanthin (Fuco), 19'-hexanoyloxyfucoxanthin (19-Hex) and chlorophyll c_3 (Chl c_3). Fuco, Chl c_3 and 19-Hex were used as chemotaxonomic proxies for diatoms and prymnesiophytes (DiTullio and Smith, 1995; DiTullio et al., 2003; Wright et al., 2010). Precision of analyses for pigments is ca. 10%, and the lower limit of detection is ca. 0.02 μg L^{-1}. The pigment19-Hex is considered to be a robust indicator of *Phaeocystis* biomass in the Ross Sea, based on the correlation between pigment concentrations and microscopically determined cell abundance (Leventer and Dunbar, 1996; Goffart et al., 2000; DiTullio et al., 2003). The proportional contribution of each group to total chlorophyll *a* concentrations was estimated by CHEMTAX (Mackey et al., 1996; Wright et al., 2010) using the characteristic phytoplankton pigment ratios of DiTullio et al. (2003).

Phytoplankton variable fluorescence was measured using a bench-top fast repitition rate fluorometer (FRRF). This instrument is equipped with an array of blue LED lights (~470 nm) with a total power of 6 W cm^{-2}. In continuous wave mode the instrument can deliver up to 8000 μmol photons m^{-2} s^{-1} while performing FRRF excitation. The FRRF excitation flashes are produced at photon flux density of ca. 65,000 μmol photons m^{-2} s^{-1}, with 150 ns rise time and 200 ns fall time. A thermo-electric cooled 10-mm photodiode detector (Advance Photonics) was connected to an elbow-shaped light pipe to collect the emission light from the bottom of the sample chamber. The instrument has a sensitivity of 0.01 μg L^{-1} chlorophyll *a* with ± 5–10% accuracy. Replicate measurements on the same sample indicated a precision of ca. 3%. The measurement protocol was optimized to obtain fluorescence saturation (F_m) by a rapid sequence of 80 flashlets, followed by 30 flashlets at exponentially increasing intervals, to characterize the relaxation kinetics of fluorescence transients. Instrument blanks were determined with distilled water to account for light scattering within the sample chamber, and with seawater that had been filtered through a Millex AA 0.8 μm Millipore Membrane to account for fluorescence of dissolved organic matter. Water samples for FRRF measurements were subsampled from the 10-L Niskin bottles, immediately placed on ice, and kept under low light (from 5–10 μmol photons m^{-2} s^{-1}) for adaptation to low light for 30–40 min. Minimal (F_o) and maximal (F_m) fluorescence and the absorption cross section of PSII were calculated from each saturation curve. Reference and baseline corrections were used to estimate other photosynthetic parameters, such as the functional absorption cross section (σ_{PSII}) (Kolber et al., 1998), which was calculated by fitting the fluorescence transient to a theoretical function describing the fluorescence–photosynthesis relationship (Kolber et al., 1998). Two FRRFs were used that differed in the LED array sizes and in the signal attenuation method, but performed similarly. Samples were either placed into the cuvette via pipettes or dispensed through the cuvette with a peristaltic pump with a maximum flow rate of 5 mL min^{-1}. To avoid condensation on the cuvette due to the temperature difference between the cold seawater and the laboratory air, the light and cuvette chambers were constantly flushed with dry nitrogen gas. Over 100 filtered seawater blanks were measured during the two cruises (Tozzi, 2010). Seawater blanks were obtained by filtering samples by applying gentle and constant pressure with a 60 mL syringe

through MF-Millipore MCE Membrane Millex AA 0.8 μm filters. The observed blanks ranged from 0.07–4.4% of the corresponding F_m signal, with an average of 0.87 ± 1.38% on samples with chlorophyll *a* concentrations ranging between 0.28 and 6.16 μg L^{-1}. Contrary to the findings of Cullen and Davis (2003), the filtered seawater blanks did not contribute substantially to the F_v/F_m

Table 1
Mean (± standard deviation), minimum (Min), and maximum (Max) values for physical and chemical water properties for cruises NPB06-01 and NBP06-08. All means represent averages from the mixed layer; PAR represents averages of each station's subsurface value.

Variable	Cruise					
	NBP06-08 (spring)			*NBP06-01 (summer)*		
	Mean	*Min*	*Max*	*Mean*	*Min*	*Max*
Temperature (°C)	−1.78 ± 0.13	−2.08	−0.97	−0.73 ± 0.86	−1.95	2.75
Salinity	34.49 ± 0.10	33.68	34.79	34.38 ± 0.16	33.89	34.81
σ_T (kg m^{-3})	27.77 ± 0.80	27.54	28.02	27.63 ± 0.15	27.07	27.98
PAR (μmol photons m^{-2} s^{-1})	454 ± 406	27.2	1350	341 ± 371	23.5	1610
Mixed layer depth (m)	65 ± 52	7	317	36 ± 26	10	179
Euphotic depth (m)	34 ± 13	17	82	26 ± 9	9	58
Nitrate (μM)	28.7 ± 1.80	23.0	33.6	23.4 ± 5.80	2.5	32.7
Phosphate (μM)	2.08 ± 0.15	1.64	2.55	1.72 ± 0.43	0.11	2.79
Silicate (μM)	82 ± 2.8	75	93	75 ± 9.5	30	106
Iron (nM)	0.08 ± 0.04	0.04	0.23	0.14 ± 0.07	0.06	0.34

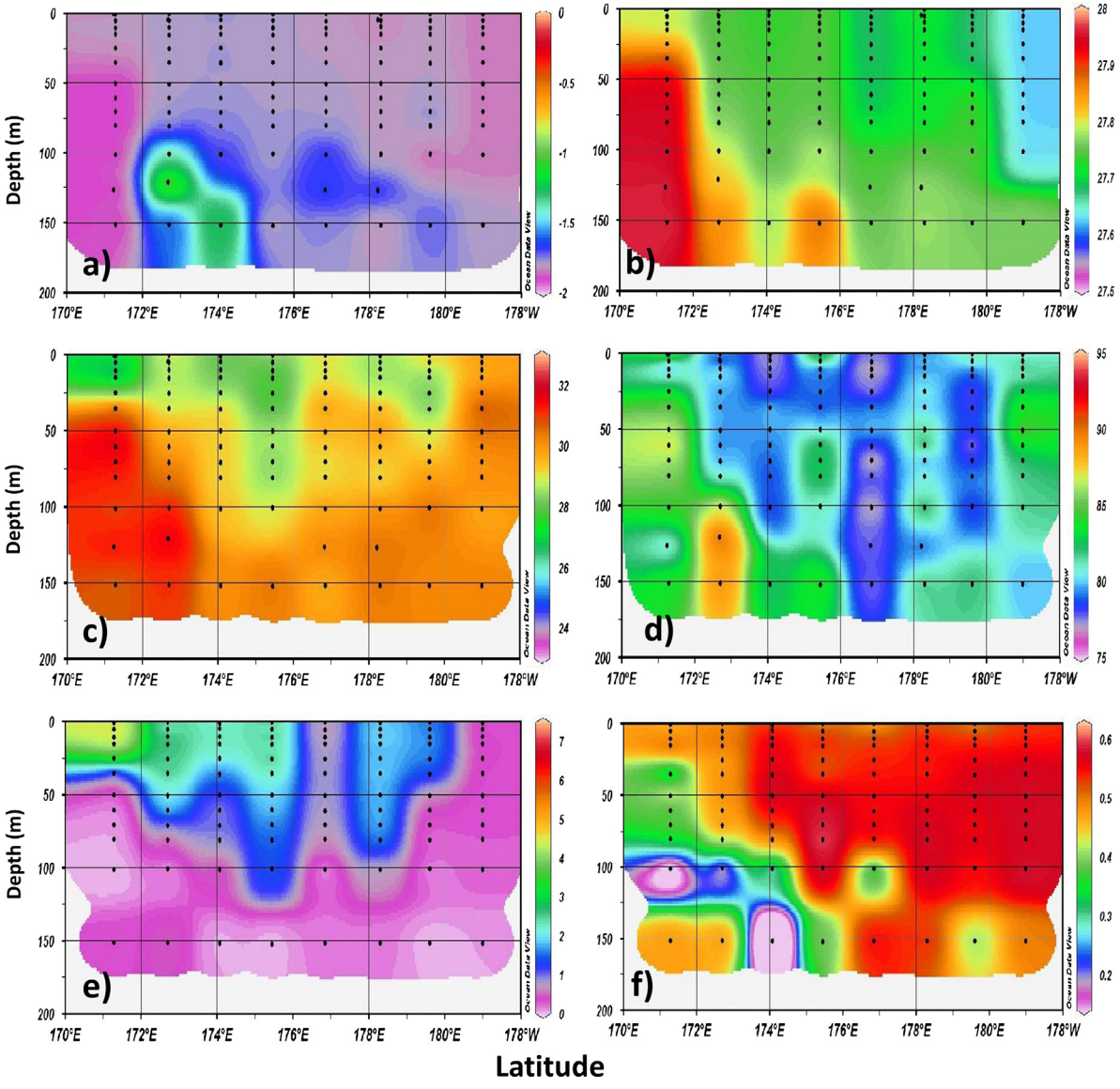

Fig. 2. Cross-section during the spring cruise (NBP06-08) at 76°S of (a) temperature, (b) density (σ_T), (c) nitrate, (d) silicic acid, (e) chlorophyll, and (f) quantum yield (F_v/F_m).

values. The FRRF was periodically blanked with a DI water sample to account for the cuvette light scattering and to monitor potential bio-fouling.

Statistical analyses were conducted using SAS software. All data are available at http://osprey.bco-dmo.org/project.cfm?flag=view&id=40&sortby=project.

3. Results

3.1. Physical and chemical features of waters from 0 to 200 m

The average mixed layer depth (z_{mix}) during the spring cruise was ~65 m, roughly 30 m deeper than during the summer cruise (Table 1). Surface salinity distribution during spring showed no spatial or temporal trends that would indicate measurable freshwater contributions to the surface waters. Mean sea surface temperatures (−1.78 °C ± 0.13) were too cold to melt substantial quantities of ice, and temperature- or salinity-induced buoyancy effects were minimal (Figs. 2–4; Long et al., 2011, 2012). Similarly, the euphotic zone (Z_{eu}, the depth at which observed irradiance was 1% of the surface value) was deeper during the spring cruise (mean of 34 m and a maximum of 82 m) than during the summer cruise (mean of 26 m and a maximum of 58 m; Table 1). Using the formula of van Hilst and Smith (2002) to estimate the mean euphotic zone irradiance with the mean PAR, mixed layer depths, and attenuation coefficients (Table 1), we estimate that the spring water columns on average experienced 56% of the irradiance of those in the summer. Macronutrients (NO_3^-, $Si(OH)_4$, and PO_4^{-3}) remained at relatively high concentrations during both the spring and summer cruises, although some nutrient removal had occurred in the euphotic zone relative to concentrations at depth. During spring, mean nitrate concentrations in the upper 10 m were reduced to 29 μM (compared to ca. 31 μM below the euphotic zone), and decreased further during summer to ~23 μM (Table 1; Fig. 5). In contrast, surface dissolved iron concentrations during the spring cruise averaged 0.08 ± 0.04 nM in the upper 40 m and were not significantly different from those during the summer cruise (mean = 0.14 ± 0.07 nM; Table 1, Fig. 8). The nutricline was approximately coincident with the base of the euphotic zone, whereas the ferricline was substantially deeper (roughly 90 m) during both cruises. Meltwater input from sea ice and glacial ice in summer created surface water that had warmed and was fresher than the deeper (ca. 150 m) waters. In all three transects of the summer cruise, there was a more uniform water column centered from 177°E-180° characterized by cooler, more saline water (Figs. 6–8). Surface mixed layer depths during summer varied from 10 to 179 m, averaging 36 m (Table 1). The deepest z_{mix} values were observed in the north along 74.5°S and in the south along 77.5°S, while the shallowest z_{mix} values were mostly found in the west, consistent with climatological means conditions (Orsi and

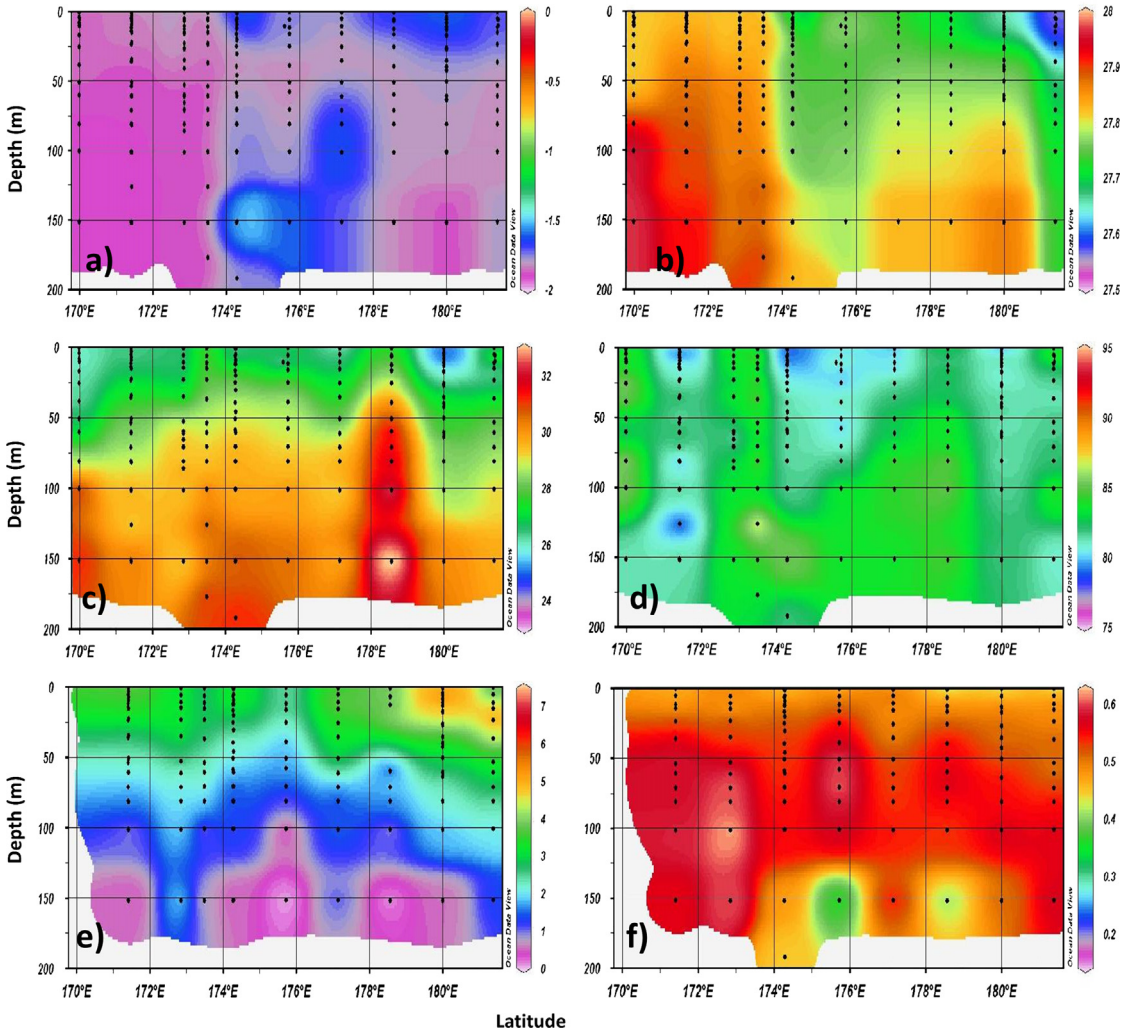

Fig. 3. Cross-section during the spring cruise (NBP06-08) at 76.5°S of (a) temperature, (b) density (σ_T), (c) nitrate, (d) silicic acid, (e) chlorophyll, and (f) quantum yield (F_v/F_m).

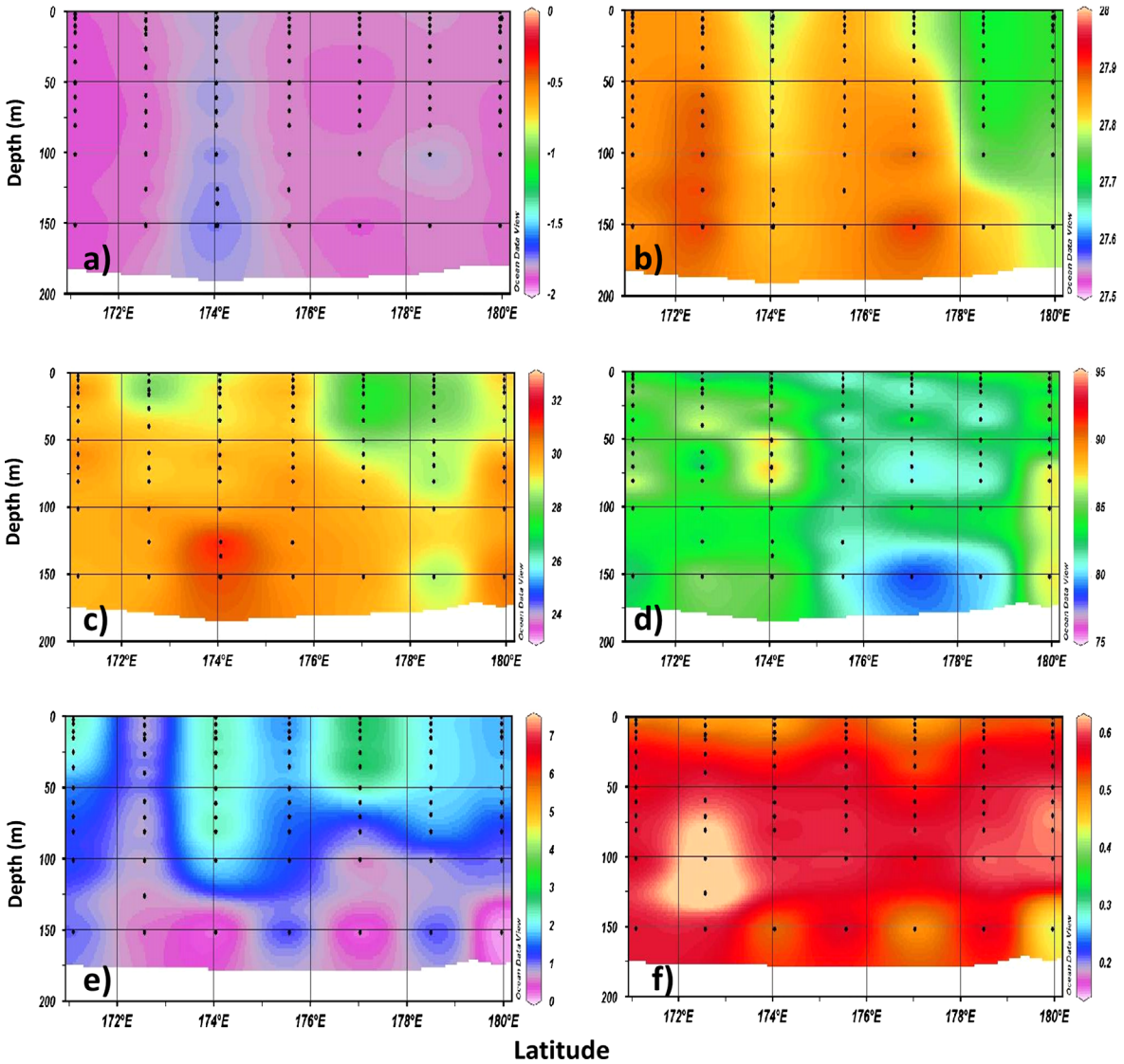

Fig. 4. Cross-section during the spring cruise (NBP06-08) at 77°S of (a) temperature, (b) density (σ_T), (c) nitrate, (d) silicic acid, (e) chlorophyll, and (f) quantum yield (F_v/F_m).

Wiederwohl, 2009). Surface PAR fluxes were not significantly different between the spring and summer cruises (Table 1).

3.2. Chlorophyll a, particulate matter and pigment concentrations

During the spring cruise we observed relatively high biomass that was dominated by *P. antarctica* colonies, with chlorophyll *a* concentrations averaging 7 μg L^{-1} at stations dominated by *P. antarctica* (data not shown). The average chlorophyll *a* concentration for all stations was 2.11 μg L^{-1} (Table 2). Along the transect at 76°S, the highest chlorophyll *a* levels were observed in the west (Fig. 2), whereas along 76.5°S maximum chlorophyll *a* concentrations were found in the east (Fig. 3). The waters along 77.5°S were characterized by relatively low biomass, with higher chlorophyll *a* levels observed in the low density ($\sigma_t < 27.78$ kg m^{-3}) surface waters at 174°E (~2.5 μg L^{-1} chl *a*) and 177°E (~3 μg L^{-1} chl *a*) (Fig. 4). The highest chlorophyll *a* concentrations were found along the Ross Ice Shelf between 175°E and 179°E and west of 172°E, with concentrations up to 7 μg L^{-1} chl *a* and negligible dissolved silicate drawdown (data not shown). Pigment analyses clearly revealed that this transect was dominated by *P. antarctica* (Fig. 9).

During the summer cruise mean chlorophyll *a* concentrations were similar to the spring values (2.11 μg L^{-1} in spring vs. 2.13 μg L^{-1} in summer; Table 2), although lateral and vertical distributions were markedly different. Chlorophyll *a* standing stocks during summer ranged from 0.03 to 7.47 μg L^{-1} in the euphotic zone. Along 76°S elevated chlorophyll *a* concentrations were observed in the east and west, but low levels were observed between 169 and 178°E (Fig. 6). Two distinct assemblages were identified, with the western side dominated by diatoms and the eastern side dominated by *P. antarctica* (Fig. 9). Chlorophyll *a* was elevated along nearly the entire 76.5°S transect (Fig. 7), except close to the ice edge in the west. In contrast, the transect at 77.5°S was characterized by relatively low chlorophyll *a* concentrations throughout (< 1.5 μg L^{-1}; Fig. 8), except for the region between 176°E and 179°W where values > 4 μg L^{-1} were observed. High biomass, up to 6 μg L^{-1} chl *a*, was found along 77.5°S at the end of December (December 29) and was dominated by *P. antarctica*, but the biomass had decreased to ~2 μg L^{-1} chl *a* two weeks later in the same location (data not shown). The percentage of chlorophyll *a* attributable to diatoms (Fig. 9) also varied with a substantial dissolved silicate reduction and accumulation of biogenic silica (Table 2). The greatest biogenic silica concentrations were observed at the most westerly stations (88, 98, 93 and 94), where the water temperatures were highest (up to 2.5 °C) and which had intermediate chlorophyll *a* concentrations of 1.5 to 2.4 μg L^{-1}. The POC and PON concentrations (averaging 10.7 and 1.76 μmol L^{-1},

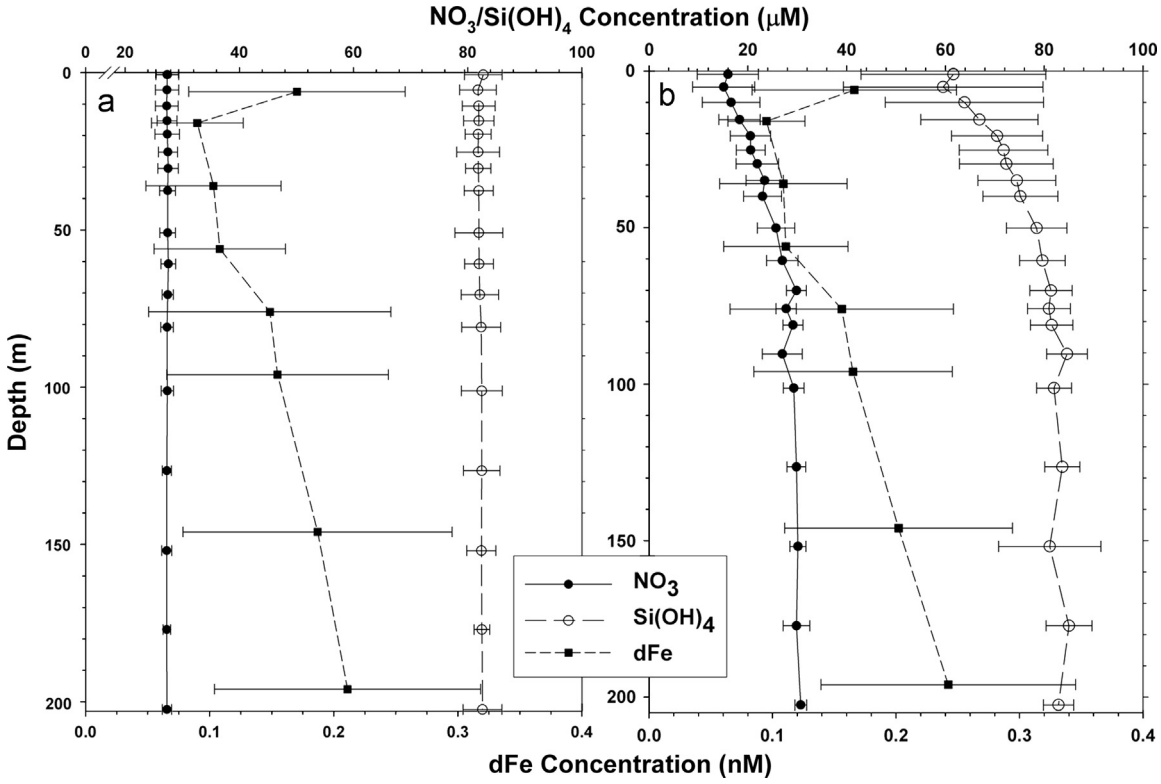

Fig. 5. Average vertical distributions and standard deviations of nitrate (black circles), silicic acid (open circles), and iron concentrations (black squares) during (a) the spring cruise (NBP11-08) and (b) the summer cruise (NBP11-01).

respectively) were also elevated during the summer cruise and paralleled increases of chlorophyll *a* (Table 2). The average BSi concentrations during summer were nearly an order of magnitude greater than during spring, although the means of both POC and PON during the summer cruise were only twice those during the spring cruise (Table 2). The BSi:POC molar ratios were three-fold higher during the summer cruise than during the spring cruise, although the POC:PON molar ratios were similar (6.80 and 6.76 in spring and summer, respectively; Table 2). In conrast, POC/chl *a* ratios were markedly higher in summer than in spring (120 vs. 49, respectively; Table 2), which we believe primarily reflects the different irradiance conditions encountered during summer.

During the spring cruise high concentrations of 19-hex were observed (mean concentration in the upper 50 m was 730 ± 742 ng L^{-1}), along with low fucoxanthin concentrations (mean of 219 ± 174 ng L^{-1}). All other accessory (non-chlorophyll) pigments (except diadinoxanthin) were present at levels less than 100 ng L^{-1}. The CHEMTAX analysis suggested that *P. antarctica* contributed nearly 85% of the total chlorophyll *a* during the spring cruise, whereas diatoms contributed only 8% (Fig. 9). During the summer cruise, however, the pigment concentrations and estimated contributions to biomass by the various phytoplankton groups were considerably different. Mean 19-hex and fucoxanthin concentrations were 489 ± 690 and 638 ± 538 ng L^{-1}, respectively, and peridinin (indicative of autotrophic dinoflagellates) concentrations exceeded 100 ng L^{-1} (mean concentrations were 136 ± 48 ng L^{-1}). Relative contributions of *P. antarctica*, diatoms and dinoflagellates to the total chlorophyll *a* were 49, 41 and 8%, respectively.

3.3. Variable fluorescence

During the spring cruise phytoplankton in the upper 50 m exhibited relatively high photosynthetic efficiencies, with F_v/F_m values between 0.5 and 0.6 at the surface (Figs. 2–4). Values greater than 0.5 generally are indicative of little or no nutrient limitation (Behrenfeld et al., 2006). Mild photoinhibition was apparent at the surface, indicated by lower F_v/F_m values, which averaged 0.48 ± 0.05 ($n=66$) in the upper 10 m. Higher quantum yields ($F_v/F_m > 0.55$) were usually found below the mixed layer (Fig. 10a). Along the transects at 76.5 (Fig. 3) and 77°S (Fig. 4), a greater surface depression was observed, with mean surface F_v/F_m values decreasing to 0.45. In general where strong vertical gradients in density were observed, parallel gradients in F_v/F_m values were also detected (e.g., 171.5°E, Fig. 4; 174 and 177°E, Fig. 5). Subsurface maxima were observed at all stations. During the summer cruise the range of F_v/F_m values was greater than that observed during the spring cruise. Along 76°S surface values were close to 0.4, and along 76.5 and 77.5°S surface F_v/F_m values decreased to near 0.35 (Figs. 6–8). As observed during spring, F_v/F_m values at depth (> 20 m) increased to levels greater than 0.5, and stations with strong density gradients exhibited pronounced F_v/F_m gradients (e.g., 168.6°E, Fig. 6; 175°E, Fig. 7). The depth of the photoinhibitory effects increased with latitude and z_{mix}. The F_v/F_m values during summer in the top 10 m averaged 0.35 (± 0.054; $n=106$), significantly less than those measured during spring, and in the upper 1 m F_v/F_m ranged between 0.23 and 0.49. The summer F_v/F_m values were highly correlated with dissolved macronutrients and temperature (Table 3), but during the spring relationships between F_v/F_m and other parameters were weaker, with only temperature and phosphate being significantly correlated with F_v/F_m (Tozzi, 2010; Liu and Smith, 2012). No significant correlation between dissolved iron concentratons and F_v/F_m was observed for the merged spring–summer data set (Fig. 11). Furthermore, no significant relationship was found between particulate Fe or total Fe concentrations and quantum yields. Functional absorbtion cross sections were greater in spring than in summer (Fig. 10b). Spatial variations in σ_{PSII} were observed, but were not significantly correlated with the distribution of any chemical or hydrographic property.

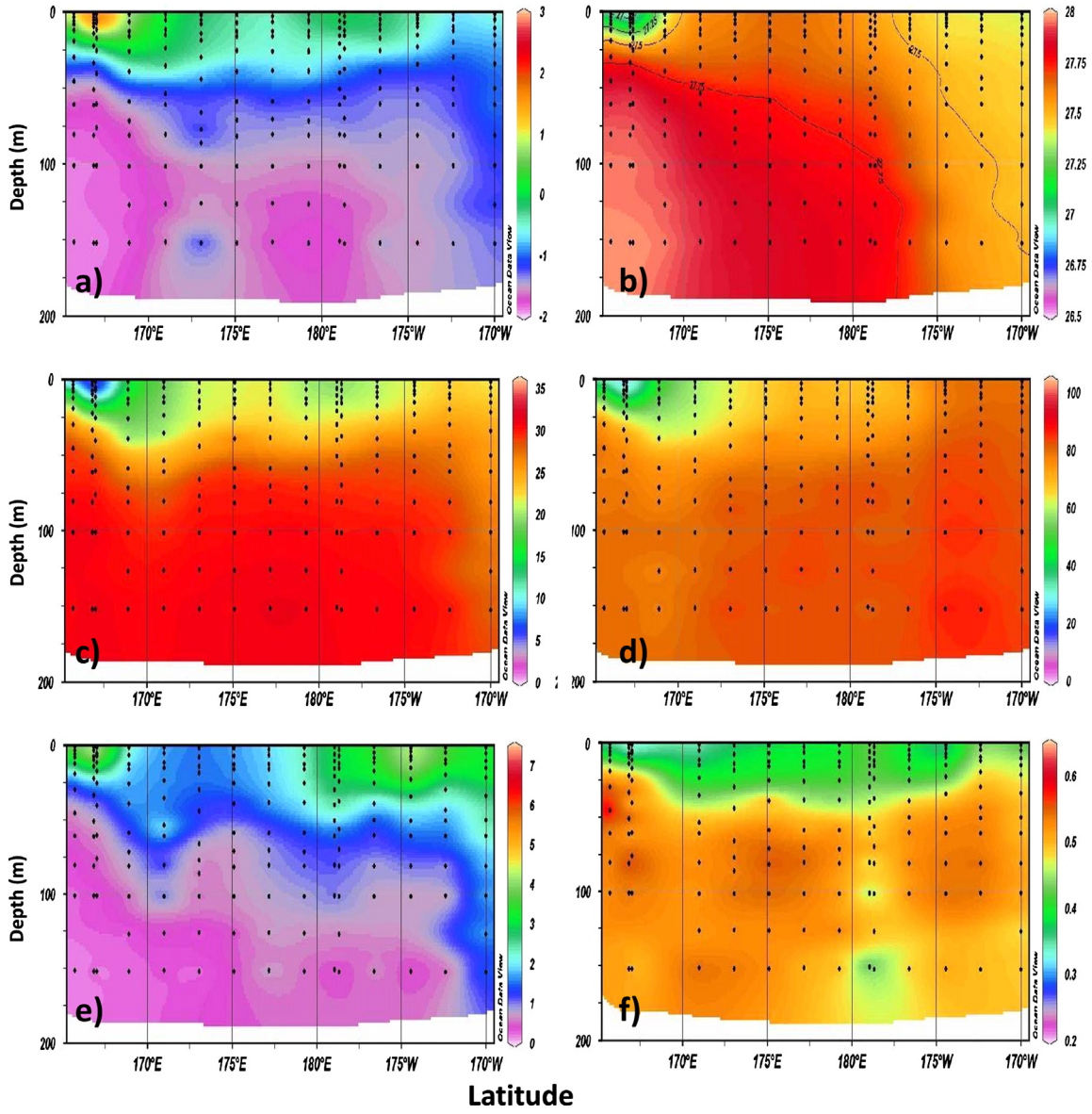

Fig. 6. Cross-section during the summer cruise (NBP06-01) at 76°S of (a) temperature, (b) density (σ_T), (c) nitrate, (d) silicic acid, (e) chlorophyll, and (f) quantum yield (F_v/F_m).

Stations from both cruises were selected as either diatom- or *Phaeocystis*-dominated based on the CHEMTAX-estimated contributions to total chlorophyll *a*, and the water column properties and photosynthetic variables for these stations compared (Fig. 12). Diatoms clearly occurred in warmer, more stratified water, and these assemblages were characterized by lower concentrations of chlorophyll *a* than those dominated by *P. antarctica*. During both cruises reduced quantum yields ($F_v/F_m \sim 0.30$) were measured in the upper water column at locations dominated by diatoms, with marked subsurface increases to 0.57. For those stations dominated by *P. antarctica*, F_v/F_m values were greater near the surface (~ 0.38) and subsurface increases more modest (~ 0.52 at depth; Fig. 12a). Water column F_v/F_m means were not significantly different. In contrast, functional absorption cross sections in the upper 40 m were significantly ($p < 0.01$; *t*-test) greater for stations dominated by diatoms relative to those dominated by *P. antarctica* (average σ_{PSII} for diatom- and *P. antarctica*-dominated stations in the upper 40 m were 1640 ± 62.2 and 1077 ± 28.1 Å^2 quantum^{-1}, respectively; Fig. 12b). Variations in σ_{PSII} as a function of depth were insignificant ($\sim 5\%$) for *Phaeocystis*-dominated assemblages, although values decreased $\sim 20\%$ at depth in diatom-dominated assemblages (Fig. 12b).

4. Discussion

Although the Ross Sea has been repeatedly shown to be the most productive region in the Southern Ocean (Arrigo et al., 2008; Smith and Comiso, 2008), our understanding of the environmental controls on phytoplankton growth and standing stocks is incomplete. Standing stocks in spring in the southern Ross Sea are nearly always characterized by a large bloom dominated by *P. antarctica* (Arrigo et al., 1999; Smith et al., 2000, 2011b); indeed, nutrient removal rates suggest that *P. antarctica* was responsible for 41% of the annual production in the three years assessed, and on average 75% during spring (Smith et al., 2011b). The dominance of *P. antarctica* in spring has been attributed to its ability to grow under low and variable irradiance in environments induced by deep vertical mixing and sea-ice cover (Kropuenske et al., 2009). Conversely, diatoms have been observed to dominate during

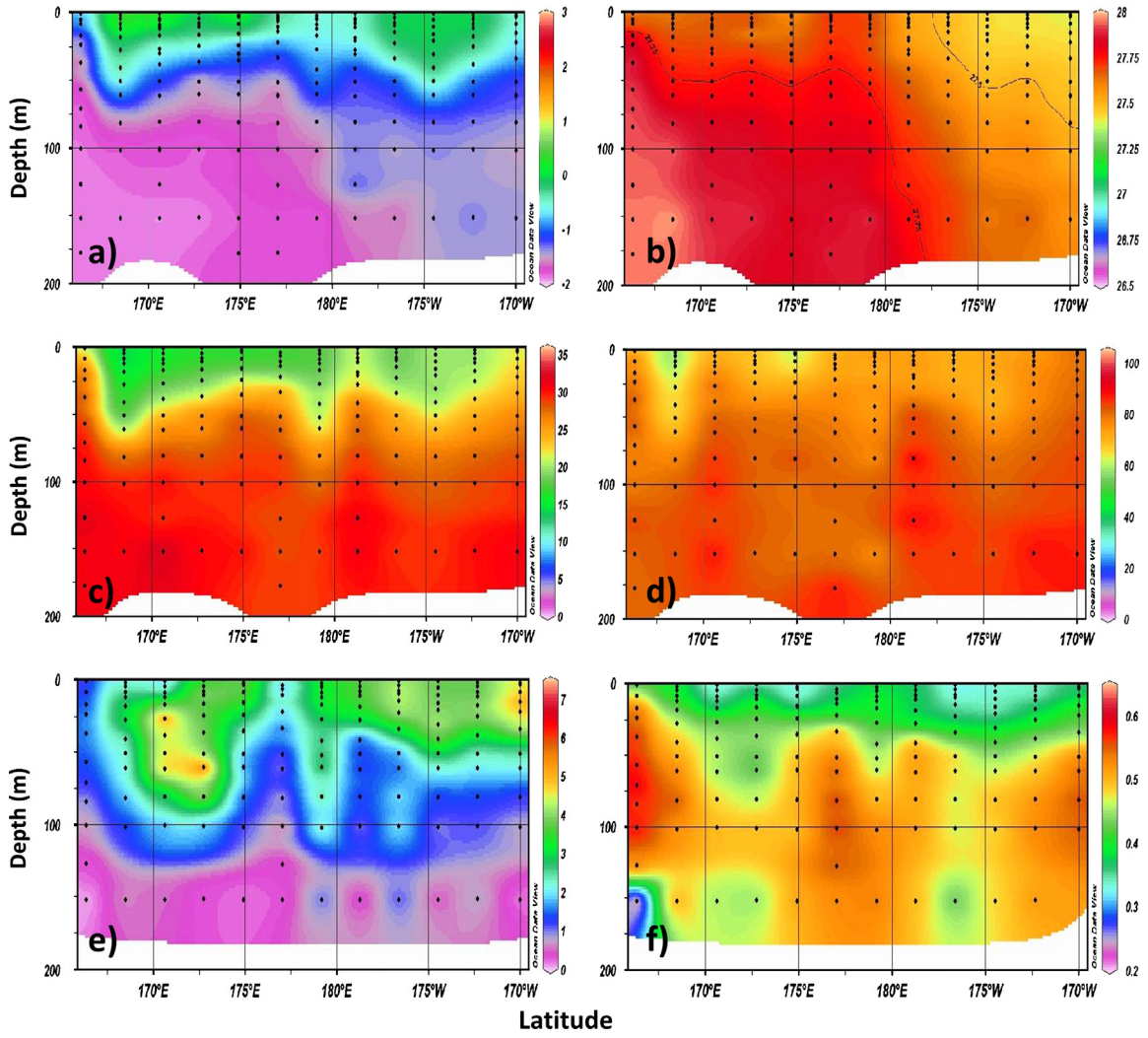

Fig. 7. Cross-section during the summer cruise (NBP06-01) at 76.5°S of (a) temperature, (b) density (σ_T), (c) nitrate, (d) silicic acid, (e) chlorophyll, and (f) quantum yield (F_v/F_m).

summer at locations with shallow mixed layers, when absolute irradiance reaches its seasonal maximum, and *P. antarctica* colonies aggregate and sink from the surface layer (Asper and Smith, 1999; Smith et al., 2011a,b). It has also been suggested that iron plays an important role in regulating phytoplankton composition (Arrigo et al., 2003). It is not known whether *Phaeocystis* and diatoms have substantially different iron uptake demands, or if their respective iron uptake capabilities are different enough to provide either with an ecological advantage. The low and likely growth-limiting iron concentrations observed during both spring and summer make it difficult to distinguish between the effects of iron and irradiance (Sedwick et al., 2011). By using active fluorescence techniques, we hoped to gain insights into the potential relationships among phytoplankton composition, photosynthesis, iron concentrations, and irradiance; nonetheless, our results suggest that iron concentrations, while likely influencing quantum yields, were not significantly correlated with them over the entire seasonal cycle, presumably due to the low dissolved iron levels observed (Sedwick et al., 2011). Indeed, our results indicate the role of irradiance in regulating photophysiology in the Ross Sea. Our findings are similar to those reported by Feng et al. (2009) in manipulations of Ross Sea phytoplankton assemblages under controlled iron and light conditions, and who also found that irradiance dominated the changes in F_v/F_m and that iron had only a modest impact on quantum yield. Differences related to assemblage composition (diatoms vs. *P. antarctica*) were observed, although those also may be coupled to changes in the environment that supported the growth and emergence of each dominant functional group.

The observed relationship between dissolved iron distribution and phytoplankton quantum yields was complex, despite the well established functional relationship between iron abundance and photosynthetic quantum yields in other areas of the ocean (Behrenfeld et al., 2006; Moore et al., 2007). No significant relationship in the merged spring–summer data set was found between F_v/F_m and dissolved iron concentrations. A possible explanation is that this may reflect temporal decoupling between quantum yields and iron concentrations in this non-equilibrium ecosystem; that is, elevated iron levels may reflect conditons where growth had only recently been initiated, hence quantum yields were low. The lack of relationship may also suggest the importance of the relationship between iron and irradiance under low irradiance conditions; that is, acclimation to low irradiance requires the synthesis of additional chlorophyll and photosynthetic enzymes and membranes, which in turn requires additional iron (Sunda and Huntsman, 1997; Boyd and Abraham, 2001). Another possibility is that particulate iron might be an important source of biologically available iron that is not reflected in the measured dissolved Fe concentrations; that is, dissolved iron concentrations do not reflect the potentially rapid uptake and

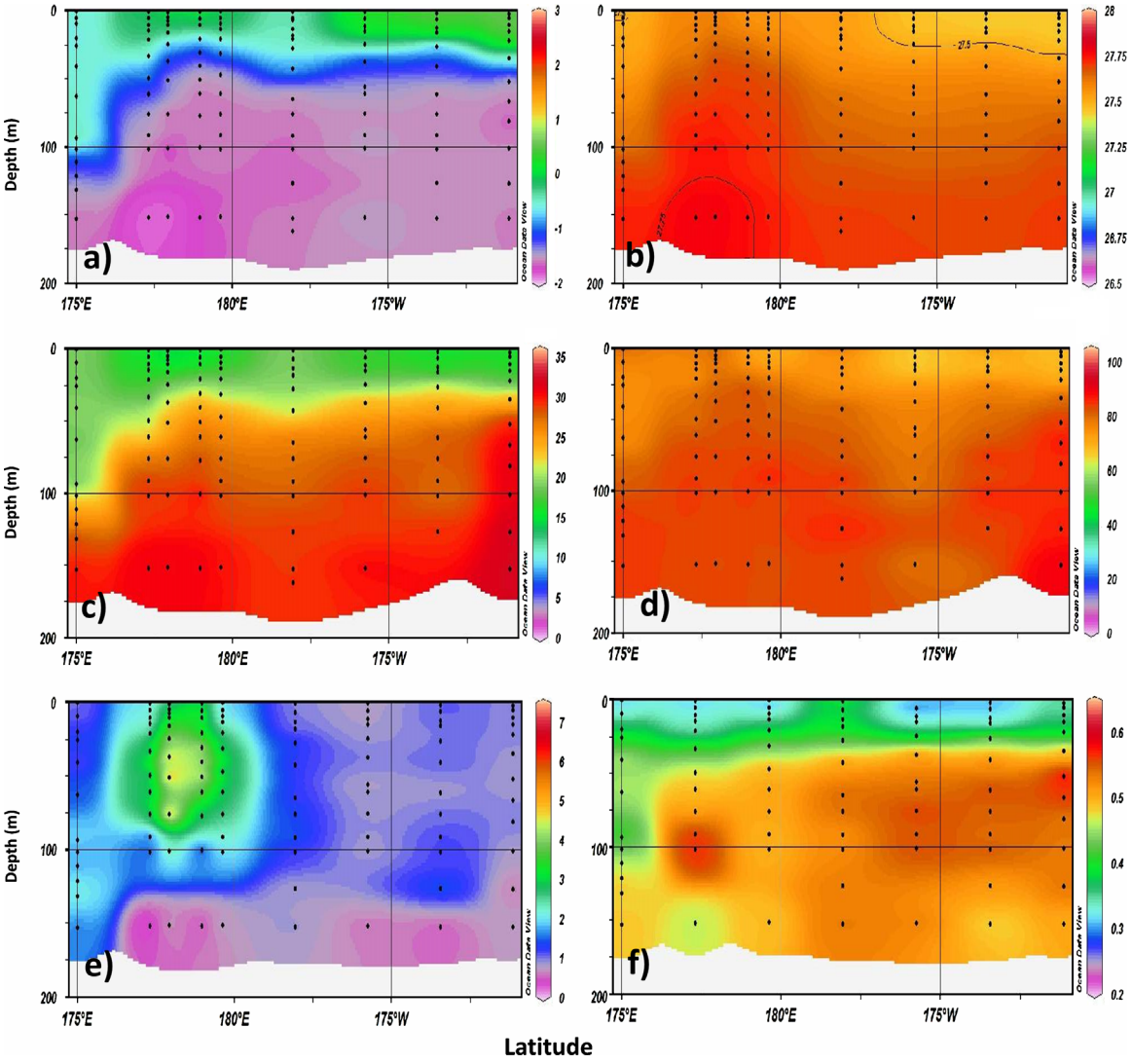

Fig. 8. Cross-section during the summer cruise (NBP06-01) at 77.5°S of (a) temperature, (b) density (σ_T), (c) nitrate, (d) silicic acid, (e) chlorophyll, and (f) quantum yield (F_v/F_m).

Table 2
Mean ($\pm$ standard deviation), minimum (Min), and maximum (Max) values for various particulate matter properties for cruises NPB06-01 and NBP06-08. Chlorophyll *a* (Chl *a*) values determined by HPLC. Percentages of *P. antarctica* and diatom chlorophyll were derived from CHEMTAX pigment analysis. nd = not detectable.

Variable	Cruise					
	Spring, NBP06-08			*Summer, NBP06-01*		
	Mean $\pm$ *Standard Deviation*	*Min*	*Max*	*Mean* $\pm$ *Standard Deviation*	*Min*	*Max*
Chl *a* ($\mu g\ L^{-1}$)	2.11 ± 1.61	0.00	7.29	2.13 ± 0.86	0.034	7.47
Particulate organic carbon ($\mu mol\ L^{-1}$)	10.7 ± 7.79	1.55	29.3	21.7 ± 9.69	1.21	61.5
Particulate organic nitrogen ($\mu mol\ L^{-1}$)	1.76 ± 1.10	0.20	4.88	3.44 ± 1.73	0.12	10.1
Biogenic silica ($\mu mol\ L^{-1}$)	0.58 ± 0.46	0.051	2.91	5.92 ± 4.50	0.037	22.3
Mean BSi:POC ratio (m/m)	0.068 ± 0.032	0.014	0.27	0.22 ± 0.14	0.0064	0.85
Mean POC:PON ratio (m/m)	6.80 ± 1.58	15.8	5.14	6.74 ± 0.86	4.97	11.7
Mean POC/chl ratio (w/w)	49.3 ± 26.4	12.2	262	121 ± 65.7	36.3	543
P. antarctica chl (% of total)	84.6 ± 12.3	29.4	98.6	49.2 ± 30.3	nd	70.2
Diatom chl (% of total)	8.41 ± 7.95	nd	47.9	41.4 ± 26.8	nd	87.6

turnover of the bioavailable pool due to the use of particulate and/or biological recycling. Such availability of particulate Fe, perhaps involving photoreduction or recycling of Fe, might also be strongly seasonal. In addition, in summer pCO_2 is drawn down to low levels ($< 150\ \mu atm$) in the Ross Sea, which increased seawater pH. Shi et al. (2010) have suggested that pH could regulate the biological availability of iron, much of which is organically complexed, which could complicate the relationship between quantum yield

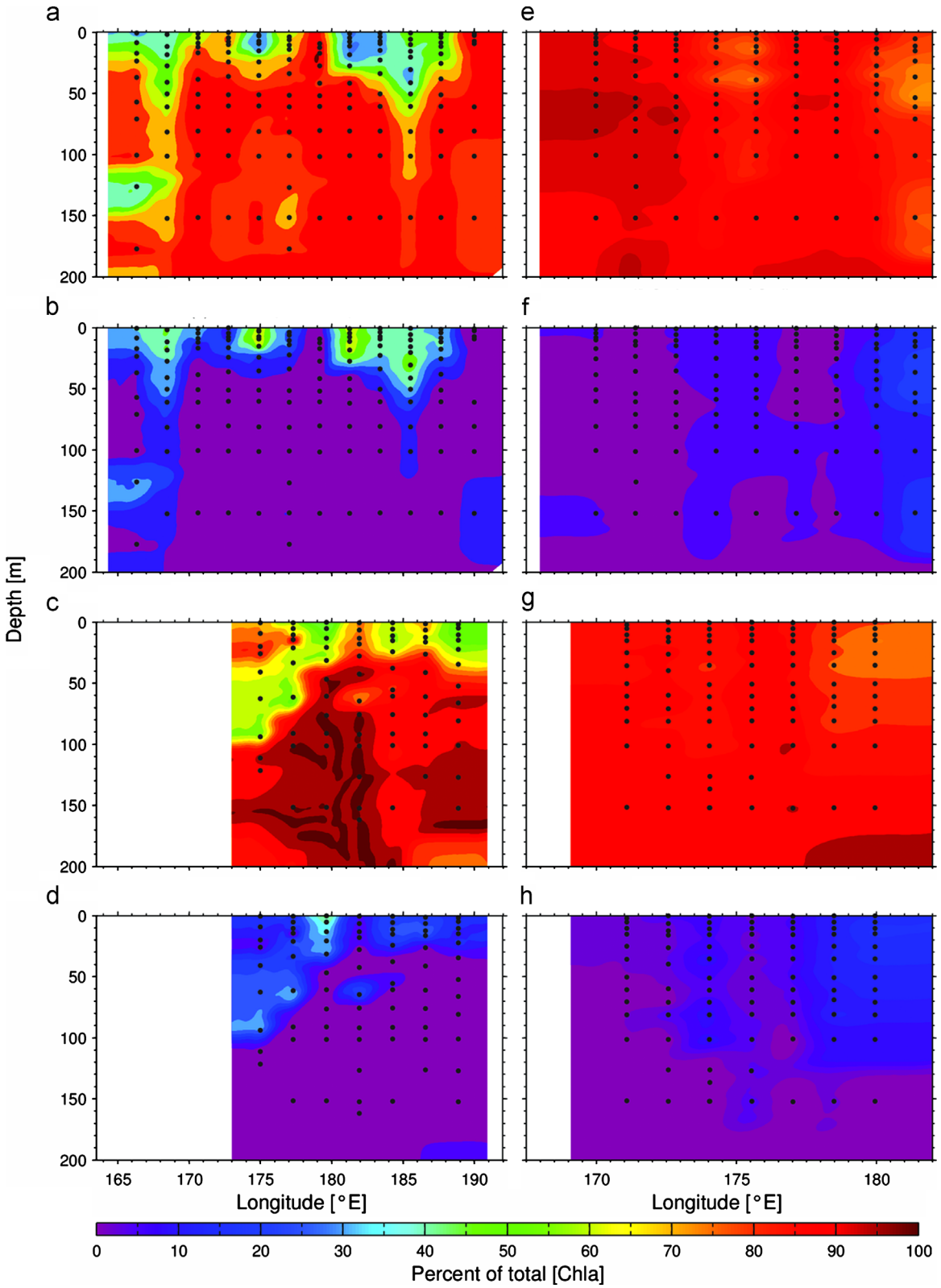

Fig. 9. Distribution of the per cent contribution to total chlorophyll of *P. antarctica* (a,c,e,g) and diatoms (b,d,f,h) during summer cruise (NBP06-01; panels a,b,c,d) and spring cruise (NBP06-08; panels e,f,g,h) at 76.5°S (panels a,b,e,f), and 77.5°S (panels c,d,g,h). White areas indicate no data.

and dissolved iron in the Ross Sea. Breitbarth et al. (2010) reported that increased seawater pH resulted in increased iron availability. Finally, F_v/F_m values are impacted by other environmental factors, such as irradiance, which might mask any relationship between quantum yields and dissolved iron concentrations. In cultures at low irradiances, the iron requirement for growth is increased due to the requirements of chlorophyll *a* synthesis (Sunda and Huntsman, 1997; Maldonado et al., 1999; Garcia et al., 2009; Alderkamp et al., 2012a), whereas the effects on natural assemblages within a mixed layer are less well known (Boyd and Abraham, 2001).

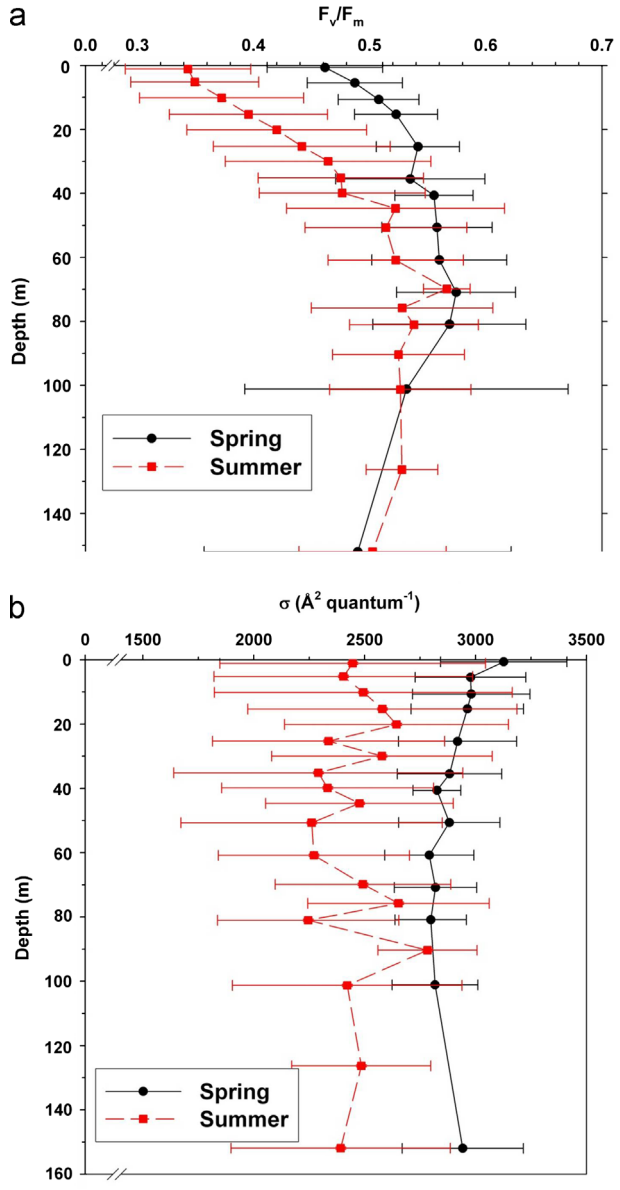

Fig. 10. Vertical distribution of (a) quantum yield (F_v/F_m) and (b) absorption cross section (σ_{PSII}) as a function of depth during the spring (NBP06-08; •) and summer cruises (NBP-6-01; ■).

The horizontal and vertical distributions of quantum yield exhibited substantial variations (Figs. 2–4, 6–9). However, there are only a limited number of spatial observations on a similar scale as ours to compare with the magnitude of the changes we observed. For example, Bibby et al. (2008) assessed variations in both quantum yield and absorption coefficients in eddies in the waters off Hawaii and Bermuda, and found that elevated chlorophyll *a* levels associated with eddies generally had reduced F_v/F_m values. Within a single eddy, F_v/F_m generally was reduced at the surface and increased with depth and became maximal just below the deep chlorophyll *a* maximum. This pattern was attributed to severe nutrient limitation at the surface, and increased nutrient availability at depth (Kolber et al., 1990; Greene et al.,1991; Geider et al., 1993). Quantum yields reported by Bibby et al. (2008) showed the same range of values that we measured in the Ross Sea (Fig. 10a). Based on the vertical distribution of dissolved iron (dFe) and F_v/F_m in our study, we can most likely eliminate the possibility of the F_v/F_m maximum resulting from dFe vertical inputs, since the ferricline was substantially deeper and surface inputs are spatially restricted. Bibby et al. (2008) also measured the σ_{PSII} and found they averaged ca. 475 Å^2 quantum^{-1} in all of the eddies, only 36% of the values we measured in the Ross Sea; they also argued that quantum yields and functional absorption cross sections were inversely correlated, and suggested that this relationship indicated nutrient limitation. We found no clear correlation between F_v/F_m and σ_{PSII}, again suggesting the secondary role of nutrient limitation in the Ross Sea and the importance of irradiance. The measured σ_{PSII} values were higher in spring than in summer throughout the water column (Fig. 10b), which may reflect slightly decreased dFe availability, but this might also reflect the influence of increased irradiance availability and/or assemblage composition. Behrenfeld and Kolber (1999) reported σ_{PSII} values to range from 200 to 1000 in the tropical Pacific and Atlantic Oceans, again lower than values we measured in the Ross Sea. We did observe a significant difference in σ_{PSII} values between diatoms and *P. antarctica*-dominated assemblages, which may reflect a number of responses. First, *P. antarctica* was largely dominant during spring, a period of reduced stratification and colder temperatures, whereas the relative aboundance of diatoms increaese throughout the summer, and they were overwhelmingly dominant under conditions of increased stratification, enhanced mean irradiance (such as in the shallowest mixed layers) and warmer water temperatures. It is possible that diatoms have a greater ability to utilize non-photochemical quenching in situ that allows for the dissipation of excess absorbed energy. Secondly, *P. antarctica* undergoes substantial pigment packaging, which may influence the efficiency of photon absorption (Moisan et al., 1998; Moisan and Mitchell, 1999); it also produced myccosporine-like amino acids, which can protect against ultraviolet radiation (Moisan et al., 2010). We conclude that the differences in photochemical characteristics we observed between the two major functional groups were largely driven by irradiance, although we cannot identify the specific physiological mechanism(s) that drive this difference.

We were unable to identify a single environmental factor responsible for the dominance of diatoms or *P. antarctica* in the Ross Sea polynya. Macronutrients rarely limit production (Tremblay and Smith, 2007); instead, the hypothesis that the spatial and temporal distribution of phytoplankton is driven by iron and light availability and by differences in photophysiology and resource utilization appears to be strongly supported (Arrigo et al., 1999; Olson et al., 2000; Kropuenske et al., 2009). Diatom-dominated blooms are mostly confined to shallow mixed layers and warmer waters during summer, a conclusion also supported by a substantially larger data set and statistical analysis (Liu and Smith, 2012). Vertical structure of variable fluorescence-derived parameters, highlighted by the persistent photoinhibition of surface phytoplankton, suggests suboptimal in situ photosynthetic rates and primary production during summer (Smith et al., 2000), while in spring photoinhibition was found only along the ice shelf in waters with higher biomass, possibly indicating irradiance and micronutrient co-limitation (Sunda and Huntsman 1997; Boyd et al., 1999). A significant relationship between iron concentrations and F_v/F_m values was absent, despite the well established relationship between iron concentration, photosynthetic quantum yields and productivity (Olson et al., 2000; Behrenfeld et al., 2006; Moore et al., 2007). The consistently high photosynthetic quantum yields below the mixed layer both in spring and summer suggests full acclimation of all subsurface populations to low light. The quantum yields in summer were significantly reduced in the upper water column where macro- and micronutrients were most reduced. A correlation of the vertical distribution of F_v/F_m during the spring cruise with temperature, with lower values in warmer waters, also is most likely due to the same type of co-limitation,

Table 3
Means, standard deviatons, and ranges of fluorometric chlorophyll *a* (Chl *a*), dissolved macronutrients (N, Si, P), temperature and dissolved iron (dFe) during the spring and summer cruises for *all* samples where quantum yield (F_v/F_m) was measured. Results of simple linear correlations between quantum yield and same variables are also provided (m=slope, b=intercept, r^2=correlation coefficient, and p=probability of regressions). Quantum yield for all samples averaged 0.533 ± 0.050 (range 0.355–0.646) in spring and 0.490 ± 0.095 (range 0.204–0.618) in summer.

Variable	Mean ± standard deviation	Minimum	Maximum	b	m	r^2	p
NBP 06-08 (spring)							
Chl *a* (μg L^{-1})	1.59 ± 1.39	0.01	7.30	0.57	−0.02	0.06	0.07
NO_3^- (μM)	28.2 ± 1.88	23.0	32.8	0.073	0.02	0.04	0.09
$Si(OH)_4$ (μM)	81.8 ± 2.83	75.9	93.6	0.44	0.001	0.06	0.74
PO_4^{-3} (μM)	2.04 ± 0.15	1.64	2.37	0.20	0.16	0.24	0.040
T (°C)	−1.79 ± 0.45	−2.08	1.90	0.16	−0.21	0.11	0.006
dFe (nM)	0.11 ± 0.06	0.06	0.24	0.63	−1.05	0.52	< 0.001
NBP 06-01 (summer)							
Chl *a* (μg L^{-1})	1.59 ± 1.40	0.04	5.84	3.47	−3.84	0.07	0.04
NO_3^- (μM)	25.3 ± 4.86	16.3	32.4	10.5	30.3	0.35	< 0.001
$Si(OH)_4$ (μM)	75.9 ± 8.89	54.1	89.0	54.9	42.8	0.20	< 0.001
PO_4^{-3} (μM)	1.83 ± 0.38	1.12	2.35	0.67	2.37	0.75	< 0.001
T (°C)	−1.14 ± 0.75	−1.90	0.80	1.28	−0.09	0.39	< 0.001
dFe (nM)	0.18 ± 0.10	0.06	0.53	0.200	−0.05	0.002	0.71

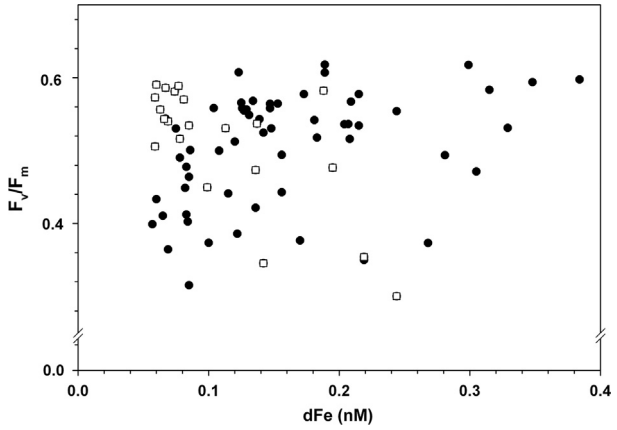

Fig. 11. Relationship between quantum yield (F_v/F_m) and dissolved iron concentrations during the spring (NBP06-08; □) and summer (NBP-6-01; •) cruises.

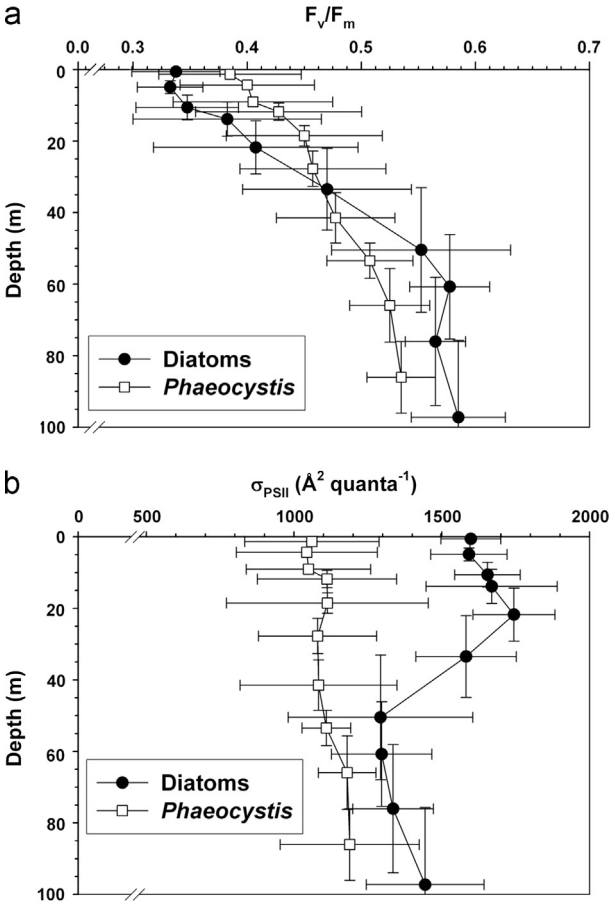

Fig. 12. Vertical distribution of (a) quantum yield (F_v/F_m) and (b) the absorption cross section (σ_{PSII}) as a function of assemblage composition. The ten stations with the largest proportional contribution to chlorophyll *a* were analyzed regardless of season sampled.

given that warmer waters were confined to surface layers in which nutrients were reduced to a greater extent and irradiance was higher. The nutrient and temperature ranges during the spring cruise were narrow, while the quantum yield vertical structure was relatively homogenous, with consistently high values reflecting the mostly deep mixed layers and indicating no major stressor or limiting photosynthetic factor.

Nonetheless, the high quantum yields and high biomass accumulation observed in November suggests relatively high growth rates and primary productivity combined with low grazing and loss rates, as demonstrated previously (Smith et al., 2000; Caron et al., 2000). Diatom dominance in summer in shallow mixed layers with increased stratification and higher temperatures is consistent with their ability to adapt to higher irradiance levels, whereas *P. antarctica* dominated in deeper mixed layers in spring when iron availability is sufficient to satisfy their iron requirements (Coale et al., 2004; Sedwick et al., 2007). Higher functional absorption cross section found in diatom-dominated surface waters during the summer is possibly an indicator of Fe stress (Berges et al., 1996; Holeton et al., 2005). *P. antarctica* had faster rates of photorecovery (Tozzi, 2010), potentially conferring an advantage in the deeply mixed waters. In summer, especially in shallow mixed layers with fewer light fluctuations, diatoms have a distinct competitive advantage due to their higher photosynthetic capacity (Kropuenske et al., 2009; Alderkamp et al., 2012a) and possibly have a reduced lower absolute Fe requirement due to reduced levels of pigments. These characteristics may allow diatoms to efficiently utilize micronutrients at the low concentrations observed in summer in the Ross Sea (an average of 0.14 in the mixed layer, Table 1; K_μ values for clutured diatoms range from 0.19 to 1.1 nM; Timmermans et al., 2004), while potentially

displaying faster growth rates with less photoadaptation stress. Being able to link the taxonomic photophysiological responses to the measured photosynthetic activity in the context of the environmental conditions is a significant step towards a better understanding of the phytoplankton dynamics in the polynya. Further measurements of iron concentrations in the Ross Sea will provide insights on the sources and mechanisms controlling the bioavalable iron and facilitate the interpretation of photophysiological data.

The data presented are valuable when considering the many difficulties of remote sensing techniques for this area. For example, as nutrient fields for the polynya and for any other oceanic regions are impossible to retrieve remotely, hydrography can only be estimated from remotely sensed ice and wind data and with the support of numerical circulation models, and chlorophyll *a* concentrations and fluorescence measurements from satellite can be limited for this region by extensive cloud and ice coverage. Despite these limitations, the Ross Sea has been a focus of research for over a century, yet many questions remain unanswered, especially those involving the characterization of the physical–biological interactions in the polynya and their effects on the biogeochemistry of the region Smith et al. (2012). These unanswered questions are even more compelling when considering the climate changes that the Ross Sea and the entire Southern Ocean as a whole are undergoing. Further research is clearly needed to address these complexities.

Acknowledgments

This research was supported by grants from the National Science Foundation (OPP-0338157 and OPP-0087401 to WOS, OPP-0338164 to PS, OPP 0741411 and 1043748 to DAH and OPP-0338097 to GRD). We thank all our CORSACS co-workers for assistance in the field, and J. Dreyer for laboratory analyses. This paper is Contribution No.3285 of the Virginia Institute of Marine Science, The College of William & Mary.

References

Alderkamp, A.-C., Kulk, G., Buma, A.C., Visser, R.J.W., van Dijken, G.L., Mills, M.W., Arrigo, K.R., 2012a. The effect of iron limitation on the photophysiology of *Phaeocystis antarctica* (Prymnesiophyceae) and *Fragilariopsis cylindrus* (Bacillariophyceae) under dynamic irradiance. J. Phycol. 48, 45–59.

Alderkamp, A.-C., Mills, M.W., van Dijken, G.L., Laan, P., Thuróczy, C.-E., Gerringa, L.J.A., de Baar, H.J.W., Payne, C.D., Visser, R.J.W., Buma, A.G.J., Arrigo, K.R, 2012b. Iron from melting glaciers fuels phytoplankton blooms in the Amundsen Sea (Southern Ocean): phytoplankton characteristics and productivity. Deep-Sea Res. II 71–76, 32–48.

Arrigo, K.R., Robinson, D., Worthen, D., Dunbar, R., DiTullio, G.R., van Woert, M., Lizotte, M., 1999. Phytoplankton community structure and drawdown of nutrients and CO_2 in the Southern Ocean. Science 283, 365–367.

Arrigo, K.R., Worthen, D.L., Robinson, D.H., 2003. A coupled ocean-ecosystem model of the Ross Sea: 2. Iron regulation of phytoplankton taxonomic variability and primary production. J. Geophys. Res., 108, http://dx.doi.org/10.1029/2001JC000856.

Arrigo, K.R., van Dijken, G., Long, M., 2008. Coastal Southern Ocean: a strong anthropogenic CO_2 sink. Geophys. Res. Lett. 35 (L21602), http://dx.doi.org/10.1029/2008GL035624.

Asper, V.L., Smith Jr., W.O., 1999. Particle fluxes during austral spring and summer in the southern Ross Sea (Antarctica). J. Geophys. Res. 104, 5345–5360.

Behrenfeld, M.J., Kolber, Z.S., 1999. Widespread iron limitation of phytoplankton in the South Pacific Ocean. Science 283, 840–843.

Behrenfeld, M.J., Worthington, K., Sherrell, R.M., Chavez, F.P., Strutton, P., McPhaden, M., Shea, D.M., 2006. Controls on tropical Pacific Ocean productivity revealed through nutrient stress diagnostics. Nature 442, 1025–1028.

Berges, J.A., Charlebois, D.O., Mauzerall, D.C., Falkowski, P.G., 1996. Differential effects of nitrogen limitation on photosynthetic efficiency of Photosystems I and II in microalgae. Plant Physiol. 110, 689–696.

Bibby, T.S., Gorbunov, M.Y., Wyman, K.W., Falkowski, P.G., 2008. Photosynthetic community responses to upwelling in mesoscale eddies in the subtropical North Atlantic and Pacific Oceans. Deep-Sea Res. II 55, 1310–1320.

Boyd, P.W., Abraham, E.R., 2001. Iron-mediated changes in phytoplankton photosynthetic competence during SOIREE. Deep-Sea Res. II 48, 2529–2550.

Boyd, P.W., et al., 2000. A mesoscale phytoplankton bloom in the polar Southern Ocean stimulated by iron fertilization. Nature 407, 695–702.

Boyd, P.W., LaRoche, J., Gall, M., Frew, R., McKay, R.M.L., 1999. Role of iron, light, and silicate in controlling algal biomass in subantarctic waters SE of New Zealand. J. Geophys. Res. 104, 13395–13408.

Breitbarth, E., Bellerby, R.J., Neill, C.C., Ardelan, M.V., Meyerhöfer, M., Zöllner, E., Croot, P., Riebesell, U., 2010. Ocean acidification affects iron speciation during a coastal seawater mesocosm experiment. Biogeosciences 7, 1065–1073.

Brzezinski, M.A., Nelson, D.M., 1995. The annual silica cycle in the Sargasso Sea near Bermuda. Deep-Sea Res. 42, 1215–1237.

Caron, D.A., Dennett, M.R., Lonsdale, D.J., Moran, D.M., Shalapyonok, L., 2000. Microzooplankton herbivory in the Ross Sea, Antarctica. Deep-Sea Res. II 47, 3249–3272.

Coale, K.H., et al., 2004. Southern Ocean iron enrichment experiment: carbon cycling in high- and low-Si waters. Science 304, 408–414.

Coale, K.H., Gordon, R.M., Wang, X., 2005. The distribution and behavior of dissolved and particulate iron and zinc in the Ross Sea and Antarctic circumpolar current along 170°W. Deep-Sea Res. I 52, 295–318.

Cullen, J.J., Davis, R.F., 2003. The blank can make a big difference in oceanographic measurements. Limnol. Oceanogr. Bull. 12, 29–35.

de Baar, H.J.W., de Jong, J.T.M., Nolting, R.F., Timmermans, K.R., van Leeuwe, M.A., Bathmann, U., Rutgers van der Loeff, M., Sildam, J., 1999. Low dissolved Fe and the absence of diatom blooms in remote Pacific waters of the Southern Ocean. Mar. Chem. 66, 1–34.

Dinniman, M.S., Klinck, J.M., Smith Jr., W.O., 2003. Cross-shelf exchange in a model of Ross Sea circulation and biogeochemistry. Deep-Sea Res. II 50, 3103–3120.

Dinniman, M.S., Klinck, J.M., Smith Jr., W.O., 2011. A model study of Circumpolar Deep Water on the West Antarctic Peninsula and Ross Sea continental shelves. Deep-Sea Res. II 58, 1508–1523.

DiTullio, G.R., Geesey, M.E., 2002. Photosynthetic pigments in marine algae and bacteria. In: Bitton, G. (Ed.), The Encyclopedia of Environmental Microbiology. John Wiley & Sons, New York, pp. 2453–2470.

DiTullio, G.R., Geesey, M.E., Leventer, A., Lizotte, M.P., 2003. Algal pigment ratios in the Ross Sea: implications for CHEMTAX analysis of Southern Ocean data. In: DiTullio, G.R., Dunbar, R.B. (Eds.), Biogeochemistry of the Ross Sea. American Geophysical Union, Washington, D.C., pp. 279–293, Antarctic Research Series 78.

DiTullio, G.R., Smith Jr., W.O., 1995. Relationship between dimethylsulfide and phytoplankton pigment concentrations in the Ross Sea, Antarctica. Deep-Sea Res. I 42, 873–892.

Dunbar, R.B., Arrigo, K.R., Lutz, M., DiTullio, G.R., Leventer, A.R., Lizotte, M.P., Van Woert, M.P., Robinson, D.H., 2003. Non-Redfield production and export of marine organic matter: a recurrent part of the annual cycle in the Ross Sea, Antarctica. In: DiTullio, G.R., Dunbar, R.B. (Eds.), Biogeochemistry of the Ross Sea. American Geophysical Union, Washington, D.C., pp. 179–195, Antarctic Research Series 78.

Feng, Y., Hare, C.E., Rose, J.M., Handy, S.M., DiTullio, G.R., Lee, P., Smith Jr., W.O., Peloquin, J., Tozzi, S., Sun, J., Zhang, Y., Dunbar, R.B., Long, M.C., Sohst, B., Hutchins, D., 2009. Interactive effects of CO_2, irradiance and iron on Ross Sea phytoplankton. Deep-Sea Res. I 57, 368–383.

Garcia, N.S., Sedwick, P.N., DiTullio, G.R., 2009. Influence of irradiance and iron on the growth of colonial Phaeocystis antarctica: implications for seasonal bloom dynamics in the Ross Sea, Antarctica. Aquat. Microb. Ecol. 57, 203–220.

Geider, R.J., Greene, R.M., Kolber, Z., MacIntyre, H.L, Falkowski, P.G., 1993. Fluorescence assessment of the maximum quantum efficiency of photosynthesis in the western North Atlantic. Deep-Sea Res. I 40, 1205–1224.

Goffart, A., Catalano, G., Hecq, J.H., 2000. Factors controlling the distribution of diatoms and *Phaeocystis* in the Ross Sea. J. Mar. Syst. 27, 161–175.

Greene, R.M., Geider, R.J., Falkowski, P.G., 1991. Effect of iron limitation on photosynthesis in a marine diatom. Limnol. Oceanogr. 36, 1772–1782.

Hiscock, M.R., Lance, V.P., Apprill, A.M., Johnson, Z., Bidigare, R.R., Mitchell, B.G., Smith Jr., W.O., Barber, R.T., 2007. Photosynthetic maximum quantum yield increases are an essential component of Southern Ocean phytoplankton iron response. Proc. Natl. Acad. Sci. USA 105, 4775–4780.

Holeton, C.L, Nédélec, F., Sanders, R., Brown, L., Moore, C.M., Stevens, D.P., Heywood, K.J., Statham, P.J., Lucas, C.H., 2005. Physiological state of phytoplankton communities in the Southwest Atlantic sector of the Southern Ocean, as measured by fast repetition rate fluorometry. Polar Biol. 29, 44–52.

JGOFS, 1996. Protocols for the Joint Global Ocean Flux Study (JGOFS) core measurements. IOC SCOR Report 19. Bergen, Norway.

Johnson, K.S., et al., 2007. Developing standards for dissolved iron in seawater. EOS Trans. Am. Geophys. Union 88, 131–132.

Kolber, Z.S., Barber, R.T., Coale, K.H., Fitzwater, S.E., Greene, R.M., Johnson, K.S., Lindley, S., Falkowski, P.G., 1994. Iron limitation of the phytoplankton photosynthesis in the equatorial Pacific Ocean. Nature 371, 145–149.

Kolber, Z., Prasil, O., Falkowski, P.G., 1998. Measurements of variable chlorophyll fluorescence using fast repetition rate techniques: defining methodology and experimental protocols. Biochim. Biophys. Acta 1367, 88–106.

Kolber, Z.S., Wyman, K.D., Falkowski, P.G., 1990. Natural variability in photosynthetic energy conversion efficiency: a field study in the Gulf of Maine. Limnol. Oceanogr. 35, 72–79.

Kropuenske, L.R., Mills, M.M., Van Dijken, G.L., Bailey, S., Robinson, D.H., Welschmeyer, N.A., Arrigo, K.R., 2009. Photophysiology in two major Southern Ocean

phytoplankton taxa: photoprotection in *Phaeocystis antarctica* and *Fragilariopsis cylindrus*. Limnol. Oceanogr.—Methods 54, 1176–1196.
Leventer, A., Dunbar, R.B., 1996. Factors influencing the distribution of diatoms and other algae in the Ross Sea. J. Geophys. Res. 101, 18489–18500.
Liu, X., Smith Jr., W.O., 2012. A statistical analysis of the controls on phytoplankton distribution in the Ross Sea, Antarctica. J. Mar. Syst. 94, 135–144.
Long, M.C., Dunbar, R.B., Tortell, P.D., Smith Jr., W.O., Mucciarone, D.A., DiTullio, G.R., 2011. Vertical structure, seasonal drawdown, and net community production in the Ross Sea, Antarctica. J. Geophys. Res. 116, C10029, http://dx.doi.org/10.1029/2009JC005954.
Long, M.C., Thomas, N., Dunbar, R.B., 2012. Control of phytoplankton bloom inception in the Ross Sea, Antarctica, by Ekman restratification. Global Biogeochem. Cycles 26, GB1006, http://dx.doi.org/10.1029/2010GB003982.
Mackey, M.D., Mackey, D.J., Higgins, H.W., Wright, S.W., 1996. CHEMTAX—a program for estimating class abundances from chemical markers: application to HPLC measurements of phytoplankton. Mar. Ecol. Progr. Ser. 144, 265–283.
Maldonado, M.T., Boyd, P.W., Harrison, P.J., Price, N.M., 1999. Co-limitation of phytoplankton growth by light and Fe during winter in the NE subarctic Pacific Ocean. Deep-Sea Res. II 46, 2475–2485.
Martin, J.H., Fitzwater, S.E., Gordon, R.M., 1990b. Iron deficiency limits phytoplankton growth in Antarctic waters. Global Biogeochem. Cycles 4, 5–12.
Martin, J.H., Gordon, R.M., Fitzwater, S.E., 1990a. Iron in Antarctic waters. Nature 345, 156–158.
Measures, C.I., Vink, S., 2001. Dissolved Fe in the upper waters of the Pacific sector of the Southern Ocean. Deep-Sea Res. II 48, 3913–3941.
Measures, C.I., Yuan, J., Resing, J.A., 1995. Determination of iron in seawater by flow injection analysis using in-line preconcentration and spectrophotometric detection. Mar. Chem. 50, 3–12.
Moisan, T.A., Mitchell, B.G., 1999. Photophysiological acclimation of Phaeocystis antarctica Karsten under light limitation. Limnol. Oceanogr. 44, 247–258.
Moisan, T.A., Neale, P., Goes, J., 2010. Mycosporine-like amino acids in phytoplankton: biochemistry, physiology, and optics. In: Kersey, W.T., Munger, S.P. (Eds.), Marine Phytoplankton. Nova Science, New York, pp. 119–143, Chapter 4.
Moisan, T.A., Olaizola, M., Mitchell, B.G., 1998. Xanthophyll cycling in Phaeocystis: changes in cellular absorption, fluorescence and photoprotection. Mar. Ecol. Progr. Ser. 169, 113–121.
Moore, C.M., Seeyave, S., Hickman, A.E., Allen, J.T., Lucas, M.I., Planquette, H., Pollard, R.T., Poulton, A.J., 2007. Iron-light interactions during the CROZet natural iron bloom and EXport experiment (CROZEX) I: phytoplankton growth and photophysiology. Deep-Sea Res. II 54, 2045–2065.
Olson, R.J., Sosik, H.M., Chekalyuk, A.M., Shalapyonok, A., 2000. Effects of iron enrichment of phytoplankton in the Southern Ocean during late summer: active fluorescence and flow cytometric analyses. Deep-Sea Res. II 47, 3179–3200.
Orsi, A.H., Wiederwohl, C.L., 2009. A recount of Ross Sea waters. Deep-Sea Res. II 56, 778–795.
Parkhill, J.P., Maillet, G., Cullen, J.J., 2001. Fluorescence-based maximal quantum yield for PSII as a diagnostic of nutrient stress. J. Phycol. 37, 517–529.
Sedwick, P.N., Bowie, A.R., Trull, T.W., 2008. Dissolved iron in the Australian sector of the Southern Ocean (CLIVAR-SR3 section): meridional and seasonal trends. Deep-Sea Res. I 55, 911–925.
Sedwick, P.N., DiTullio, G.R., 1997. Regulation of algal blooms in Antarctic shelf waters by the release of iron from melting sea ice. Geophys. Res. Lett. 24, 2515–2518.
Sedwick, P.N., DiTullio, G.R., Mackey, D.J., 2000. Iron and manganese in the Ross Sea, Antarctica: seasonal iron limitation in Antarctic shelf waters. J. Geophys. Res. 105, 11321–11336.
Sedwick, P.N., Garcia, N.S., Risemen, S.F., Marsay, C.M., DiTullio, G.R., 2007. Evidence for high iron requirements of colonial *Phaeocystis antarctica* at low irradiance. Biogeochemistry 83, 83–97.
Sedwick, P.N., Marsay, C.M., Aguilar-Islas, A.M., Lohan, M.C., Sohst, B.M., Long, M.C., Arrigo, K.R., Dunbar, R.B., Saito, M.A., Smith, W.O., DiTullio, G.R., 2011. Early-season depletion of dissolved iron in the Ross Sea polynya: implications for iron dynamics on the Antarctic continental shelf. J. Geophys. Res. 116, C12019, http://dx.doi.org/10.1029/2010JC006553.
Shi, D.L., Xu, Y., Hopkinson, B.M., Morel, F.M.M., 2010. Effect of ocean acidification on iron availability to marine phytoplankton. Science 327, 676–679.
Smith Jr., W.O., Asper, V.L., 2001. The influence of phytoplankton assemblage composition on biogeochemical characteristics and cycles in the southern Ross Sea, Antarctica. Deep-Sea Res. I 48, 137–161.
Smith Jr., W.O., Asper, V., Tozzi, S., Liu, X., Stammerjohn, S.E., 2011a. Continuous fluorescence measurements in the Ross Sea Antarctica: Scales of variability. Progr. Oceanogr. 88 28–45.
Smith Jr., W.O., Comiso, J.C., 2008. The influence of sea ice on primary production in the Southern Ocean: a satellite perspective. J. Geophys. Res. 113, C05S93, http://dx.doi.org/10.1029/2007JC004251.
Smith Jr., W.O., Marra, J., Hiscock, M.R., Barber, R.T., 2000. The seasonal cycle of phytoplankton biomass and primary productivity in the Ross Sea, Antarctica. Deep-Sea Res. II 47, 3119–3140.
Smith Jr., W.O., Sedwick, P.N., Arrigo, K.R., Ainley, D.G., Orsi, A.H., 2012. The Ross Sea in a sea of change. Oceanography 25, 44–57.
Smith Jr., W.O., Shields, A.R., Dreyer, J.C., Peloquin, J., Asper, V., 2011b. Interannual variability in vertical export in the Ross Sea: magnitude, composition, and environmental correlates. Deep-Sea Res. I 58, 147–159.
Smith Jr., W.O., Shields, A.R., Peloquin, J., Catalano, G., Tozzi, S., Dinniman, M.S., Asper, V., 2006. Biogeochemical budgets in the Ross Sea: variations among years. Deep-Sea Res. II 53, 815–833.
Sunda, W.G., Huntsman, S.A., 1997. Interrelated influence of iron, light and cell size on marine phytoplankton growth. Nature 390, 389–392.
Timmermans, K.R., van der Wagt, B., de Baar, H.J.W, 2004. Growth rates, half-saturation constants, and silicate, nitrate, and phosphate depletion in relation to iron availability of four large, open-ocean diatoms from the Southern Ocean. Limnol. Oceanogr. 49, 2141–2151.
Tozzi, S., 2010. Photobiological Studies of Ross Sea Phytoplantkon. College of William and Mary, Williamsburg, VA p. 183, Ph.D. Dissertation.
Tremblay, J.-E., Smith Jr., W.O., 2007. Phytoplankton processes in polynyas. In: Smith Jr., W.O., Barber, D.G. (Eds.), Polynyas: Windows to the World's Oceans. Elsevier, Amsterdam, pp. 239–270.
van Hilst, C.M., Smith Jr., W.O., 2002. Photosynthesis/irradiance relationships in the Ross Sea, Antarctica, and their control by phytoplankton assemblage composition and environmental factors. Mar. Ecol. Progr. Ser. 226, 1–12.
Welschmeyer, N.A., 1994. Fluorometric analysis of chlorophyll a in the presence of chlorophyll b and phaeopigments. Limnol. Oceanogr. 39, 1985–1992.
Wright, S.W., van den Enden, R.L., Pearce, I., Davidson, A.T., Scott, F.J., Westwood, K.J., 2010. Phytoplankton community structure and stocks in the Southern Ocean (30–80°E) determined by CHEMTAX analysis of HPLC pigment signatures. Deep Sea Res. II 57, 758–778.